Experimental and theoretical study of Ti-6Al-4V to 220 GPa

S. G. MacLeod, B. E. Tegner, H. Cynn, W. J. Evans, J. E. Proctor, M. I. McMahon, and G. J. Ackland

Phys. Rev. B **85**, 224202 — Published 7 June 2012

DOI: 10.1103/PhysRevB.85.224202

An Experimental and Theoretical Study of Ti-6Al-4V to Multi-mbar Pressures

S.G. MacLeod,[1,2] B.E. Tegner,[3] H. Cynn,[4] W.J. Evans,[4]

J. Proctor,[3,*] M.I. McMahon,[3,1] and G.J. Ackland[3]

[1]*Institute of Shock Physics, Imperial College London, SW7 2AZ, UK*

[2]*Atomic Weapons Establishment, Aldermaston, Reading, RG7 4PR, UK*

[3]*SUPA, School of Physics and Astronomy,*

and Centre for Science at Extreme Conditions,

The University of Edinburgh, EH9 3JZ, UK

[4]*Lawrence Livermore National Laboratory,*

Condensed Matter and Material Division,

Physics and Life Sciences Directorate, Livermore, CA 94551 USA

(Dated: March 13, 2012)

Abstract

We report results from an experimental and theoretical study of the ternary alloy Ti-6Al-4V to 221 GPa. We observe a phase transition to the hexagonal ω-phase at approximately 30 GPa, and then a further transition to the cubic β-phase starting at 94-99 GPa. We do not observe the orthorhombic γ and δ phases reported previously in pure Ti. Computational studies show that this sequence is possible only if there is significant local atomic ordering during the compression process, yet insufficient atomic diffusion to reach the phase separated thermodynamic equilibrium state.

INTRODUCTION

The commercial and industrial importance of the two-phase titanium alloy Ti-6Al-4V (wt.%, hereafter referred to as Ti64) is well established, and its mechanical properties have been studied extensively[1,2]. Ti64 is commonly employed as a high-performance component in applications for which its combination of high strength-to-weight ratio, resistance to corrosion, and ease of machinability are highly desirable[1,2]. For those applications in which extreme conditions are prevalent, for example in the automotive, aerospace and nuclear industries, it is important to understand the effects of extreme pressure and temperature on the crystal structure, and hence the mechanical properties, of alloys such as Ti64. Somewhat surprisingly, to date Ti64 has rarely been studied under such conditions[3–6].

At ambient conditions, Ti64 crystallizes predominantly in the hexagonal-close-packed or hcp structure (space group $P6_3/mmc$, $z = 2$) and is commonly referred to as the α-phase. A much smaller fraction by volume crystallizes in the body-centered-cubic or bcc structure (space group $Im3m$, $z = 1$), known as the β-phase, around the grain boundaries. This is inconsistent with the equilibrium phase diagram which shows V to be almost insoluble in Ti at ambient temperature[8], rather it reflects the high temperature situation with vanadium-poor hcp coexisting with vanadium-enriched bcc above 950 K[8]. The alloying of substitutional and interstitial impurities increases the strength of Ti64 compared with pure Ti, with Al being the α-phase stabilizer and the dominant substitutional strengthener (see for example Peters[1]).

At room temperature (RT), the α-phase of Ti64 has been observed to transform into the ω-phase (space group $P6/mmm$, z=3) on compression to 27 GPa[3]. In this angle-dispersive X-ray diffraction (ADXRD) static high-pressure study, Chesnut *et al*[3] embedded polycrystalline samples of Ti64 in a methanol-ethanol pressure transmitting medium (PTM) and compressed to 37 GPa using a diamond anvil cell (DAC). The ω-phase structure was stable up to this highest pressure. More recently, a RT DAC study of Ti64, with no PTM present, and using energy-dispersive X-ray diffraction (EDXRD), did not observe the $\alpha \rightarrow \omega$ phase transformation up to a maximum pressure 32.4 GPa[4]. As yet, shock studies of Ti64[5–7] have observed no firm evidence for an $\alpha \rightarrow \omega$ phase transformation, up to the highest shock pressure reached (25 GPa)[6].

Pure Ti, on the other hand, has received considerable attention both experimentally (in

the static and dynamic high-pressure regimes) and theoretically. On static volume compression, Ti does not follow the $\alpha \rightarrow \omega \rightarrow \beta$ transformation sequence predicted for, and observed in, both Zr and Hf[9–12]. The transition to the ω-phase occurs at 3-9 GPa on pressure increase[13–18], and the ω-phase can be retained as a metastable phase at ambient pressure; the reverse transition back to the α phase in Ti occurs only on heating for extended periods at 380 K[13].

The $\alpha \rightarrow \omega$ transition pressure is known to be sensitive to uniaxial stress[19,20], and Errandonea *et al*[20], using DACs and ADXRD, found the RT $\alpha \rightarrow \omega$ transition pressure in Ti (with a low oxygen content of 300 ppm) increased from 4.9 GPa, when using no PTM, to 10.5 GPa when using an argon PTM. The same authors also reported that the α and ω phases coexisted over a large pressure range, and that this range also depended on the PTM employed; 7.5 GPa for no PTM and 4.4 GPa for an argon PTM. On pressure release, Errandonea *et al*[20] observed that in DACs containing the least hydrostatic environments (no PTM or an NaCl PTM), the reverse $\omega \rightarrow \alpha$ transition was observed after some hysteresis, whereas for DACs with more hydrostatic environments (a methanol-ethanol PTM or argon PTM), the ω-phase was recovered. This observation agreed with the suggestion that ω-phase retention would be possible if the uniaxial stress component of the stress tensor was smaller than the transition pressure[16].

Under shock compression, the $\alpha \rightarrow \omega$ transition in Ti has been reported to occur between 10.4 GPa and 14.3 GPa[6,21–24]. An investigation into the role played by oxygen content in the formation of the ω-phase in Ti found that a high-purity Ti sample (with oxygen content 360 ppm) transformed to the ω-phase at 10.4 GPa, whereas no phase transformation was observed for a low purity Ti sample (oxygen content 3700 ppm), shocked up to 35 GPa[6,25]. The recovered high-purity sample retained 28% of the ω-phase[6]. The suppression of the $\alpha \rightarrow \omega$ phase transformation was likely caused by the presence of interstitial oxygen, a known α-phase stabiliser[16,25].

Using DACs, Ti has been compressed at RT up to 216 GPa, and the transformation sequence $\alpha \rightarrow \omega \rightarrow \gamma \rightarrow \delta$ was reported[17,18]. Vohra *et al* loaded Ti foil (99.8% purity) into a DAC, with no PTM, and compressed to 146 GPa[17]. Analysis of the EDXRD data showed a transformation at 116(4) GPa from the ω-phase to an orthorhombic γ-phase, which has a distorted-hcp structure, space group $Cmcm$, and which was observed to be stable up to 146 GPa[17]. Using ADXRD, Akahama *et al* loaded both Ti powder (99.98% purity) and foil

(99.5%) into DACs, again with no PTM, and compressed to 216 GPa[18]. They confirmed the existence of the $\omega \rightarrow \gamma$ transition at 128 GPa, and at 140 GPa found the γ-phase to transform into the δ-phase, which has an orthorhombic, distorted-bcc structure with space group $Cmcm$, and which is stable to at least 216 GPa[18]. Although it has a distorted-bcc structure, the pressure dependence of the δ-phase did not suggest that a transition to a bcc structure would occur at still higher pressures. However, a bcc phase of Ti (the β-phase) has been observed by Ahuja *et al*[26] in a DAC experiment using NaCl as a PTM, both on pressure increase at 42 GPa, and on downloading from the orthorhombic η-phase they synthesised at high temperatures (>1000 K) above 80 GPa.

Calculations have revealed the mechanism behind the martensitic nature of the $\alpha \rightarrow \omega$ transformation in Ti[27–29] and also the effect that impurities such as oxygen have on the transition pressure[30]. In fact, Hennig *et al*[30] predict the combined effect of the substitutional impurity Al (10.7 at.%) and interstitial impurity oxygen (0.5 at.%), is to suppress the $\alpha \rightarrow \omega$ transformation in Ti64 to 63 GPa.

Most calculations of the phase transitions in Ti at 0 K predict the $\alpha \rightarrow \omega \rightarrow \gamma$ sequence[31–36] and suggest that the presence of shear forces in the DAC experiments may be causing the appearance of the metastable γ phase. The $\omega \rightarrow \gamma$ transition pressure is predicted to be 102-110 GPa[33,35,36]. However, Joshi *et al*[31] and Ahuja *et al*[26] calculated the transition from the ω to the β phase to take place at the lower pressure of 93 GPa[31] and 80 GPa[26], with no intermediate phases. In most cases the orthorhombic δ phase is calculated to be either energetically unstable, or to be formed as a consequence of the non-hydrostatic conditions present in DAC experiments[31–33,35]. The $\delta \rightarrow \beta$ transformation is predicted to occur below 200 GPa, at 161 GPa[34] and 136 GPa[32].

Our motivation for conducting the present study was to determine the role of alloying in changing the phase behaviour of Ti alloys, specifically whether Ti64 exhibits similar behaviour to that reported for pure Ti at multi-megabar pressures in transforming to the γ and δ phases, and whether there is a direct $\omega \rightarrow \beta$ transition in the alloy. To that end, we have made X-ray diffraction studies of Ti64 in a range of different PTMs to above 200 GPa. Using electronic structure calculations, we have also investigated the effects of local ordering in Ti64 by comparing the observed structural behaviour with that calculated for structures with different ordering schemes.

EXPERIMENTAL DETAILS

We sourced powdered samples of polycrystalline Ti64 from Goodfellow Metals possessing an oxygen impurity level of 0.123 wt.%. These powders were prepared using plasma atomization, a patented approach used by Goodfellow[37]. In this technique, a wire is passed through three converging plasma torch jets, with the molten droplets of metal separating from the wire and cooling in a jacketed, inert column. The rapid cooling suggests that the local ordering will be frozen-in from high temperature, and there will be insufficient time for nucleation of secondary, ordered, phases.

The samples were loaded into several membrane-driven DACs equipped with either 200 μm flat culets or 300/100 μm bevelled culets. The samples were loaded using a number of different PTMs to investigate the effects of non-hydrostaticity on the phase transition behaviour. In order of increasing hydrostaticity the PTMs were: no PTM, mineral oil, 4:1 methanol-ethanol, and neon. Cu powder was used as the pressure calibrant[38] in all experiments except for that in which Ti64 was embedded in neon, as the neon PTM could also act as the pressure marker in that case[39].

We collected RT angle-dispersive powder-diffraction data on the HPCAT (High Pressure Collaborative Access Team) beamlines 16-ID-B and 16-BM-D, at the Advanced Photon Source, Argonne National Labs. In our experiments, the monochromatic X-ray beam energy ranged between 30.4 keV and 33.0 keV (corresponding to λ = 0.40723 to 0.37571Å), and the beamsize was $\sim$5$\times$14 microns. Diffraction patterns were collected using a Mar345 image plate detector placed between 200 mm and 350 mm from the sample, and then integrated using the Fit2D[40] software package to give standard powder profiles. The integrated profiles were indexed using XRDA[41] and the unit cell parameters refined from measured peak positions using the least-squares fitting package Unitcell[42].

EXPERIMENTAL RESULTS

We compressed samples of Ti64 to 70 GPa (in a 4:1 methanol-ethanol PTM), 128 GPa (in a neon PTM), 174 GPa (no PTM) and 221 GPa (in a mineral oil PTM). In each case, a diffraction pattern taken from the sample at low pressures showed diffraction peaks from only the α-phase. On pressure increase, we found the α-phase of Ti64 started to transform

TABLE I: The observed $\alpha \rightarrow \omega$ phase transition pressure, and the zero-pressure bulk modulus and its derivative, for the α-phase of Ti64 compressed in a number of different pressure transmitting media. The results obtained in previous studies[3,4] are given for comparison.

Pressure medium	$P_{\alpha\rightarrow\omega}$ (GPa)	K_0 (GPa)	K'
No medium	32.1	151(4)	1.08(0.35)
Mineral oil	26.2	106(10)	5.07(1.23)
4:1 meth:eth	31.2	115(3)	3.22(0.22)
Neon	32.7	101(3)	4.05(0.29)
4:1 meth:eth[3]	27.3	125	2.41
No medium[4]	Not observed	154(11)	5.45(1.44)

into the ω-phase at pressures between 26 and 33 GPa, which may be related to the degree of hydrostaticity of the PTM, see Table I. However, the observed values for the $\alpha \rightarrow \omega$ transition pressure are very much more similar than those observed for the same transition in pure Ti using different PTMs[20], and this similarity, and potential small variations in the experimental setup, prevents us from quantifying with confidence a link between the transition pressure and the hydrostaticity of the pressure environment.

Figure 1 shows integrated ADXRD patterns collected from Ti64 embedded in a neon PTM as it was compressed into the ω-phase. The onset of the transition in this sample was observed at 32.7 GPa, with the appearance of the dominant (110/101) diffraction peak at $2\theta \sim 10^{\circ}$. In a second sample (also loaded in a neon PTM), the onset of the transition was observed at a pressure of 32.5 GPa. As the pressure is increased further, the (110/101) peak increases in intensity and other ω-phase peaks, such as the (001), (201), (210) and others not shown in Figure 1, begin to emerge until, at $\sim$45 GPa, the transformation is complete. The α and ω phases thus coexist over a pressure range of $\sim$10 GPa. We observed similar behaviour in all our experiments, and did not observe a large variation in the coexistence region depending on the PTM used. This behaviour is thus different to that reported by Errandonea *et al*[20] in their study of the $\alpha \rightarrow \omega$ transformation in Ti.

Our observed $\alpha \rightarrow \omega$ phase transition pressures in Ti64 are summarised in Table I, together with previous measurements. Our transition pressure for Ti64 embedded in a

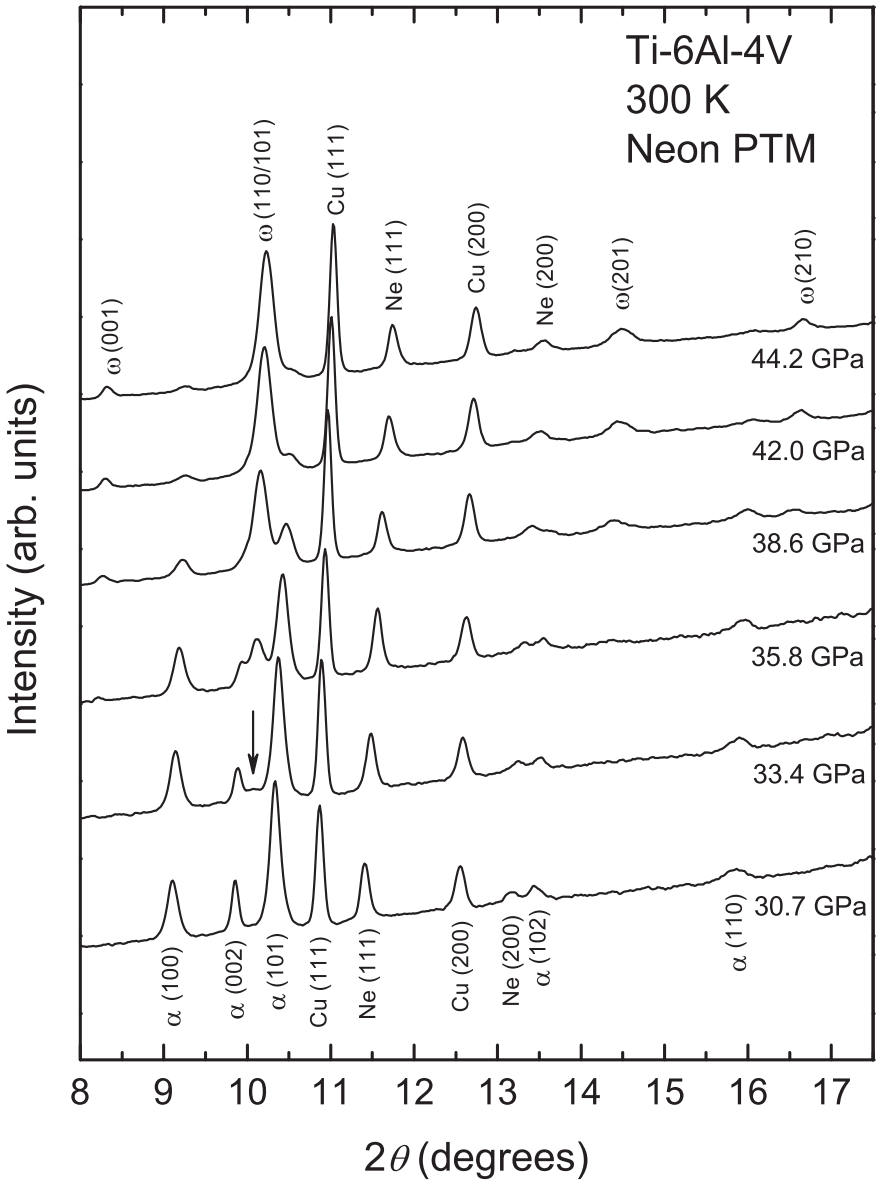

FIG. 1: Diffraction profiles collected from Ti64 on compression from 30.7 GPa to 44.2 GPa in a neon pressure transmitting medium. The arrow above the 33.4 GPa profile identifies the (110)/(101) reflection from the ω-phase, which is first evident at 32.7 GPa. Diffraction peaks from the α and ω phases, and from the Cu pressure marker and the Ne pressure medium, are indexed.

methanol-ethanol PTM is slightly higher than that obtained by Chesnut *et al*[3] using the same PTM, and our α-phase bulk modulus, $K_0 = 151(4)$ GPa when using no PTM is in agreement with the Halevy result ($K_0 = 154(11)$ GPa)[4].

We analysed the full-width at half-maximum (FWHM) of the dominant (110/101) peak at ∼41 GPa in the ω phase for all of our pressure media, and found that its width in

the least hydrostatic environment (no PTM) was 23% greater than that measured in the most hydrostatic environment (neon PTM). This broadening is a consequence of the pressure gradients and uniaxial stresses that were present in our experiments, and similar behaviour was reported previously for the (110/101) ω-phase peak in Ti under different pressure environments[20].

In all but the Ti64 loading in a methanol-ethanol PTM, compression was measured only on pressure increase. Measurements of this sample on pressure decrease from 70 GPa back to 0.8 GPa showed the ω-phase to transform completely back to the α-phase, in contrast to Errandonea *et al*[20] who recovered the ω-phase for Ti loaded into methanol-ethanol.

In three of our experiments, those using a neon PTM, mineral oil PTM and no PTM, we observed a transformation from the ω-phase to the bcc β-phase above 94 GPa. This transition is not characterised by the appearance of new diffraction peaks, such as at the α to ω transition, but rather by the gradual decrease in intensity, of the (001), (002) and (112) peaks from the ω-phase, and their subsequent disappearance. This suggests a transition to a higher-symmetry form. Figure 2 shows three diffraction patterns from Ti64 with a Cu pressure marker, but no PTM, collected at 106.3 GPa, 117.6 GPa and 127.1 GPa. At 106.3 GPa, we observe 7 clear diffraction peaks from the ω-phase. On pressure increase to 117.6 GPa there is clear evidence for the decrease in intensity of the (001), (002) and (112) peaks. Further compression to 127.1 GPa virtually completes the transformation to the bcc β-phase. We observed similar behaviour in three different samples, with the transition to the β-phase being complete between 115 GPa and 128 GPa. The volume change at the $\omega \rightarrow \beta$ transition is 0.6% for the neon PTM, 1.5% for the oil PTM and 1.6% for no PTM. This is in agreement with the $\omega \rightarrow \beta$ transition in Ti, where a two-phase refinement at 81 GPa revealed a density difference of 2%[26]; Zr, where the density difference between the ω and β phases at 30 GPa is 1.4%[10]; and Hf, where there is a volume decrease of 2.1% at the $\omega \rightarrow \beta$ transition[11].

For those experiments above 100 GPa, the pressure was increased in steps smaller than 5 GPa to ensure the detection of any intermediate phases. We found no evidence for the orthorhombic γ and δ phases reported by others in pure Ti[17,18] but only the cubic β phase, which we found to be stable to at least 221 GPa.

Figure 3 shows the c/a axial ratio for the hexagonal ω-phase over its full stability range from $\sim$30 to $\sim$125 GPa. The results obtained using no PTM and a neon PTM are identical.

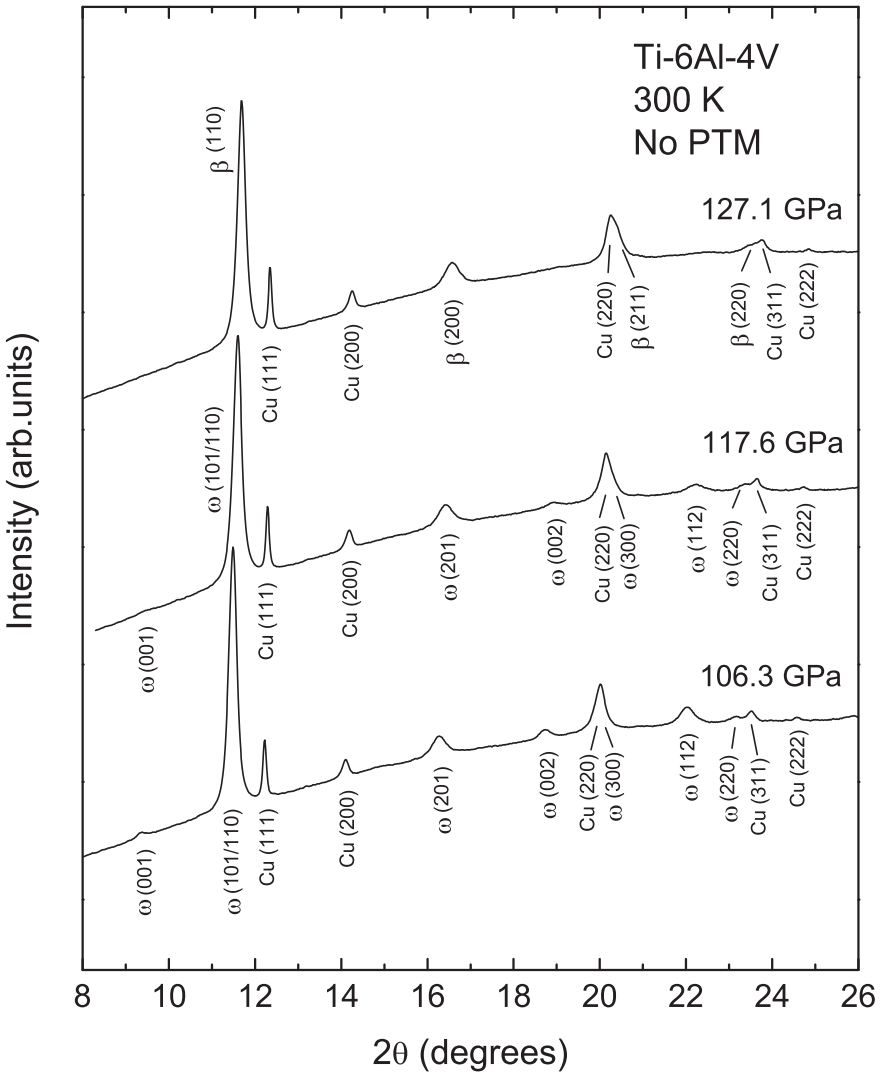

FIG. 2: Diffraction profiles collected from Ti64 on compression from 106.3 GPa to 127.1 GPa without a pressure transmitting medium, showing disappearance of the ω-phase peaks that mark the transition from the hexagonal ω-phase to the cubic β-phase. Diffraction peaks from the ω-phase and the Cu pressure marker are indexed in the 106.3 GPa profile, and peaks from the β-phase are indexed in the 127.1 GPa profile.

The axial ratio exhibits only a very small variation with pressure, and remains close to the ideal value of $\sqrt{3/8}$=0.612. As a result, the unit cell is pseudo-cubic, and the d-spacings of the (110) and (101) peaks from the ω-phase are almost identical at all pressures. The combined diffraction peaks thus remain unresolved to the highest pressures (see Fig. 2). Similar pressure independence of the c/a ratio of the ω-phase was noted previously in Zr[10], although the c/a ratio of 0.625(2), was further from the ideal value.

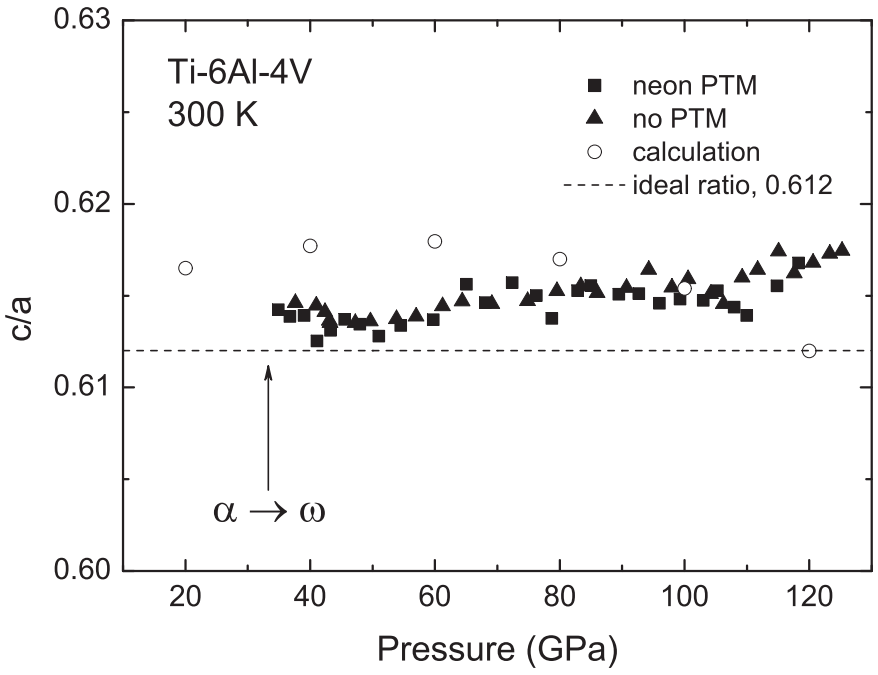

FIG. 3: Pressure dependence of the c/a ratio for the hexagonal ω-phase of Ti64, as obtained from the least (no PTM) and most (neon PTM) hydrostatic compression experiments. The calculated c/a ratio, assuming local ordering of the Al and V atoms, is shown for comparison. The horizontal dashed line indicates the "ideal" c/a ratio of $\sqrt{3/8}$ =0.612, where the hexagonal lattice is pseudo-cubic. The vertical arrow indicates the experimentally determined $\alpha \rightarrow \omega$ phase boundary

In order to determine the bulk modulus of the α-phase of Ti64, the P-V datasets were fitted using the Vinet Equation of State (EOS) formalism[43]. We measured the ambient conditions volume of Ti64 to be $V_0 = 17.252(3)$ Å^3 and fixed this value while K_0 and K' were refined. Figure 4 shows our experimental P-V data for Ti64 in a neon PTM and with no PTM present. The pressures at which the onsets of the $\alpha \rightarrow \omega$ and $\omega \rightarrow \beta$ phase transitions were detected are marked with arrows. In the case of the $\alpha \rightarrow \omega$ transition, we define this as the pressure at which the dominant (110/101) peak of the $\omega-$phase first appeared. For the $\omega \rightarrow \beta$ transition pressure, this is defined as the pressure at which the (002) and (112) peaks from the $\omega-$phase start to decrease in intensity. For Ti64 loaded with no PTM, the $\omega \rightarrow \beta$ transition begins at $\sim$94 GPa and is complete by 127 GPa. For the loading in neon, the phase-transition pressures are very similar: the ω-phase (002) and (112) peaks begin to decrease in magnitude at $\sim$99 GPa and the transformation appears to complete before 128 GPa (the highest pressure achieved in the neon experiment).

While the onset of the $\omega \rightarrow \beta$ phase transition is observed at ∼96 GPa, the complete overlap of the β phase peaks with those from the ω-phase means that the atomic volume of the β-phase can only be determined above ∼120 GPa, when it becomes the majority phase. In contrast, the additional, non-overlapping peaks of the $\omega-$phase mean that the atomic volume of this phase can be determined up to this same pressure, above which they are too weak to have their d-spacings determined accurately.

The results of our Vinet fits to the α phase are shown in Table I. For comparison, we also include the results of the two previous published DAC studies of Ti64[3,4]. There is good agreement between our results and previous results for the same pressure environments (4:1 methanol-ethanol PTM and no PTM, respectively).

COMPUTATIONAL DETAILS AND RESULTS

In order to obtain further information about the electronic and atomic structures of Ti64 we conducted extensive electronic structure calculations. These allowed us to understand the physical basis for the different phase transition sequence observed in Ti64 compared to Ti, and to investigate the effects of the local atomic ordering within the alloy.

The calculations were conducted using the plane-wave DFT-code CASTEP[44], using supercells of 54 atoms for each phase, to get impurity levels of 2 at.%. The k-point grid density for each calculation was 0.05 $Å^{-1}$. A plane-wave cut-off of 500 eV was used for basis-set convergence. A generalized gradient approximation[45] was used for the exchange-correlation. In all cases, the alloy composition was 85.2 at.% Ti, 11.1 at.% Al and 3.7 at.% V, that is, 46 atoms of Ti, 6 atoms of Al and 2 atoms of V.

The theoretical thermodynamic ground state, at ambient temperature and zero pressure, is a three-phase mixture of hcp-Ti, bcc-V and Ti_3Al, an ordered, hcp-based DO19 structure[8]. As pressure increases, only the Ti-rich phase is predicted to undergo transitions. Clearly our experimental sample, like all commercial Ti64, has not undergone this full phase decomposition, and so we assumed a single phase in the calculations.

Initially, we calculated a full set of special quasirandom structures (SQS)[46] for the binary compositions $Ti_{48}Al_6$ and $Ti_{52}V_2$ which provide a best-possible sampling of the local arrangements of the impurity atoms. In all cases calculations were carried out at constant pressure and the atoms were allowed to relax from their ideal lattice sites. Normally the crys-

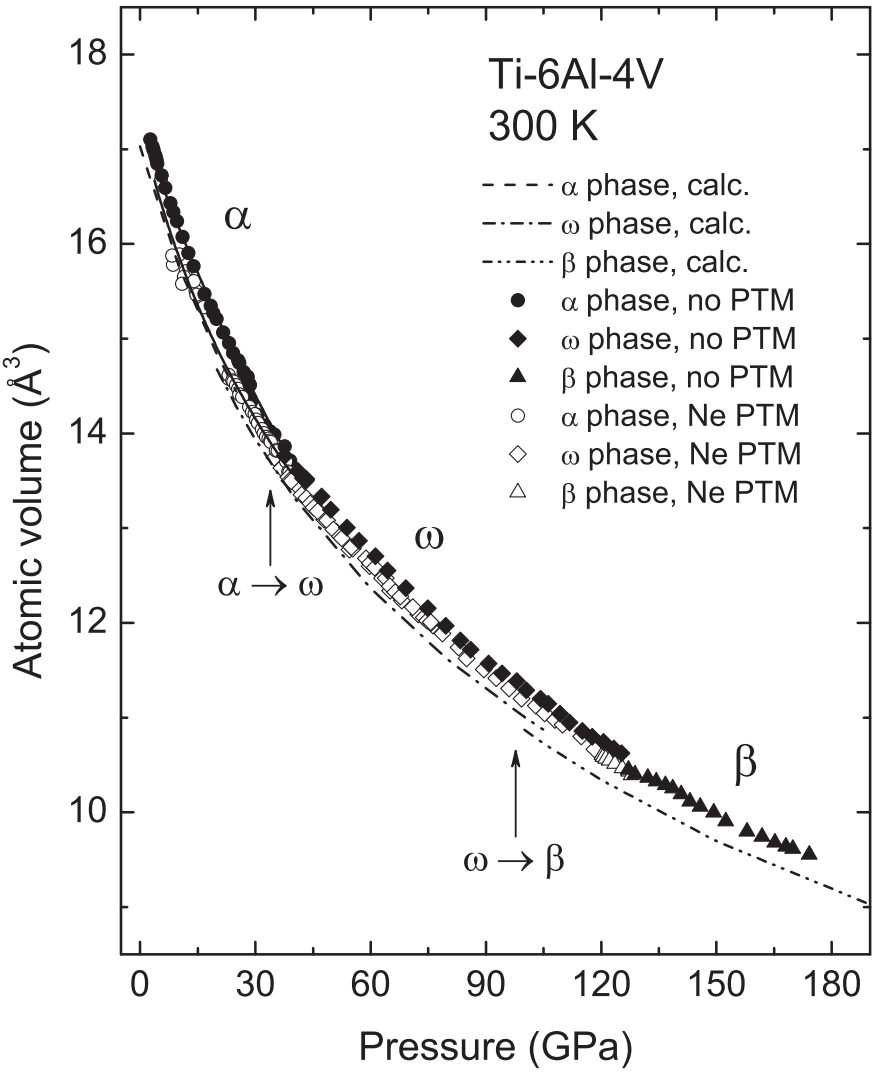

FIG. 4: The compressibility of Ti64 to 174 GPa at RT, as determined from the sample with no PTM (filled symbols), and the sample with a neon PTM (unfilled symbols). The solid line shows the Vinet fit to the α-phase data. The dashed lines shows the calculated data at 0 K, excluding thermal expansion. Peak overlap between the ω and β phases means that the atomic volume of the latter cannot be determined below $\sim$ 120 GPa - see text for details.

tal structure was preserved, but in a few cases the relaxation took the sample through the hcp-bcc transition to the more stable phase (often twinned). Such cases are easily identified and were removed from the statistics.

Analysing the calculated energies from these data showed that there was a weak tendency towards a local ordering where the minor component atoms were located as far apart as possible. At ambient pressure this effect is negligible[47] but at higher pressures it be-

comes significant, of the order 30 meV per impurity atom, with local ordering most strongly favouring the ω-phase. The primary driving force for this local ordering appears to be the oversized Al atoms. SQS samples with Al on adjacent sites have larger volumes than those with separated Al atoms, and are consequently disfavoured by high pressure.

There are several million (54!/48!/6!).1128 permutations of the atoms in the $Ti_{46}Al_6V_2$, and even the ternary alloy SQS reduction leaves an unreasonable number to calculate. So we created two samples, one set of configurations with strong local ordering (avoiding impurity near-neighbours) and another set without any ordering tendency. The comparison between these sets with the calculated enthalpies of the ω and β phases, relative to that of the α-phase, (at T=0 K) as a function of pressure are shown in Figure 5. It can be seen that the calculated transition pressures are distinctly different depending on whether local ordering is included. As we shall see, for the locally-ordered samples the calculated $\alpha \rightarrow \omega$ transition pressure is 24 GPa, in good agreement with our experimental data. The transition pressure to the β-phase is predicted to be around 105 GPa, again in good agreement with our experimental data. By contrast, if local order is excluded, then the calculations suggest that the ω-phase will not be formed at all.

The calculated c/a ratio for the ω-phase, assuming local ordering, is shown along with the experimentally-observed values in Figure 3. The agreement both in terms of the absolute value of the ratio, as well as the pressure dependence, is good. The most striking feature of this figure is the constancy of c/a over the pressure range, at precisely the value which brings the (110) and (101) diffraction peaks into coincidence. There is no symmetry equivalence between these peaks, and we attribute this locking effect to a Fermi Surface/Brillouin Zone interaction, consistent with the Hume-Rothery rules for its appearance in several materials with the same c/a ratio[48].

Above 110 GPa, we carried out calculations on pure Ti of the orthorhombic γ and δ phases[17,18]. These phases are subtle distortions away from bcc, and we successfully reproduced previous calculated results[33]. We repeated these calculations on a few representative locally-ordered supercells on Ti64, starting with the atoms on positions corresponding to ideal γ and δ-Ti. In all cases the atoms relaxed back towards the bcc positions. However, with the impurities already breaking the cubic symmetry, it is impossible to determine definitively in the calculation whether the orthorhombic distortion is absent. However, for the alloy, in all cases, we find relaxation to structures indistinguishable from those obtained

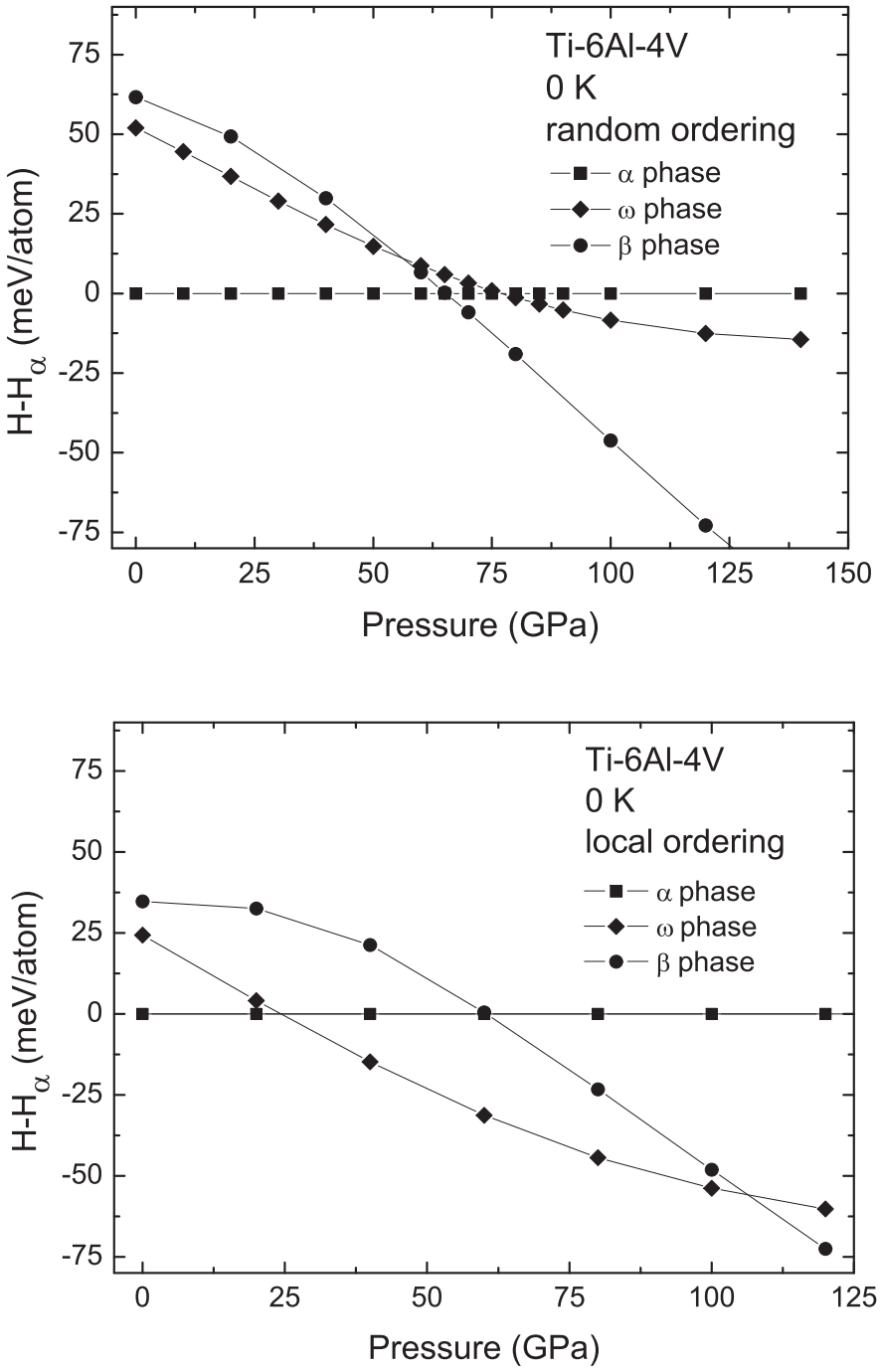

FIG. 5: The calculated enthalpy differences between the ω and β phases, relative to that of the α-phase, as a function of increasing pressure. The transition pressures are taken from where the lower curves cross. The upper graph shows the predicted transition pressures if the alloying atoms are ordered randomly, whereas the lower graph shows the transition pressures if the locations of the alloying atoms are locally-ordered so as to be distributed as far apart as possible.

starting from the cubic β-phase. This is in agreement with our non-observation of the γ and δ phases in the experiment.

CONCLUSIONS

On compression, we observe a phase transition from the ambient pressure hcp α-phase of Ti64, to the hexagonal at 26-33 GPa. This transition pressure is much higher than is the case for pure Ti (where the same transition occurs between 4.9 GPa and 10.5 GPa), and is consistent with the notion that Al is an α-phase stabilizer. The ω-phase is stable to 94-99 GPa, where there is a transition to the bcc β-phase, which in turn is stable to at least 221 GPa. This transition sequence is different to that reported for pure Ti, where there are transitions to the intermediate orthorhombic γ and δ phases[17,18]. We find no evidence either in experiment or theory for the γ or δ phases previously reported in pure Ti.

We have found that local ordering of atoms in Ti64 has significant effect on the transition pressures. DFT calculations of the $\alpha \rightarrow \omega$ and $\omega \rightarrow \beta$ transition pressures are in good agreement with experimental values only when alloying atoms are placed as far apart as possible. This ordering is primarily a volume effect due to oversized Al impurities, and only enthalpically-favoured at high pressure. We take this as evidence that pressure-induced local ordering is occurring in our high-pressure samples.

There is no thermodynamic driving force for local ordering at ambient pressure, and the samples are produced by rapid cooling from high temperature. Together, this implies that the local ordering should not have been present in the initial material. Rather, it must be created by atomic-level diffusion as the thermodynamic driving force is increased with applied pressure. Although this local diffusion occurs on the timescale of the experiment, full phase separation to thermodynamic equilibrium does not.

In contrast to a previous study[3], we observed the coexistence of the α and ω phases of Ti64 over a large pressure range. Errandonea *et al* also observed such a coexistence of these phases for pure Ti[20]. Thermodynamically, it should not be possible to have a coexistence of phases with the same chemical composition over a range of hydrostatic pressures. The observation of phase coexistence is not uncommon in DAC experiments and could well be a consequence of the non-hydrostatic conditions that frequently exist in DAC experiments, even when using a PTM such as neon. Our calculations suggest another possibility, that

the transition is not thermodynamically favoured in the absence of local ordering. Thus, the reconstructive mechanism[27] cannot operate, and the transition must take place via a much slower diffusional mechanism. The coexistence of two phases after crossing a phase boundary may be indicative of a metastable coexistence of the two phases due to kinetics. A further hypothesis, based on the thermodynamic equilibrium, is that the coexistence is due to different chemical compositions in the two phases with a higher vanadium concentration stabilising the β phase. This would require significantly more diffusion than needed for local ordering, and appears to be ruled out by the sample recovery at ambient pressure.

ACKNOWLEDGEMENTS

HPCAT is supported by CIW, CDAC, UNLV and LLNL through funding from DOE-NNSA, DOEBES and NSF. APS is supported by DOE-BES, under Contract No. DE-AC02-06CH11357. This work was performed under the auspices of the U.S. Department of Energy by Lawrence Livermore National Laboratory in part under Contract W-7405-Eng-48 and in part under Contract DE-AC52-07NA27344. Theoretical work is supported by the European project MaMiNa, which aims to develop new, more easily machinable, titanium alloys, looking at macro, micro and nano aspects. MIM is grateful to AWE Aldermaston for the award of a William Penney Fellowship.

---

* Now at: Department of Physics, University of Hull, Kingston-upon-Hull, UK

[1] M. Peters, J. Hemptenmacher, J. Kumpfert and C. Leyens, *Titanium and Titanium Alloys: Fundamentals and Applications*, edited by C. Leyens and M. Peters ,(Wiley-VCH, Weinheim, Germany, 2003), pp. 1-35.

[2] E. W. Collings, *The Physical Metallurgy of Titanium Alloys*, (Americian Society for Metals, Metals Park, Ohio, USA, 1984).

[3] G. N. Chesnut, N. Velisavljevic, and L. Sanchez, *Shock Compression of Condensed Matter - 2007*, edited by M. Elert, M. D. Furnish, R. Chau, N. Holmes, and J. Nguyen, (American Institute of Physics, New York, 2007), pp. 27-30.

[4] I. Halevy, G. Zamir, M. Winterrose, G. Sanjit, C. R. Grandini, and A. Moreno-Gobbi, *J. Phys.:*

Conf. Ser. **215**, 012013 (2010).

[5] Z. Rosenberg and Y. Meybar, *J. Phys. D: App. Phys.* **14**, 261 (1981).

[6] G. T. Gray, C. E. Morris, and A. C. Lawson, *Proceedings of Titanium '92: Science and Technology*, edited by F. H. Froes and I. L. Caplan, (Minerals, Metals and Materials Society, Warrendale, PA 15086, 1993), pp. 225-232.

[7] N. K. Bourne, J. C. F. Millett, and G. T. Gray III, *J. Mater. Sci.* **44**, 3319 (2009).

[8] F.H. Hayes, *Phase Equilib.* **16**, 163 (1995).

[9] A. Jayaraman, W. Klement, and G. C. Kennedy, *Phys. Rev.* **131**, 644 (1963).

[10] H. Xia, S. J. Duclos, A. L. Ruoff, and Y. K. Vohra, *Phys. Rev. Lett.* **64**, 204 (1990).

[11] H. Xia, H. L. Parthasarathy, Y. K. Vohra, and A. L. Ruoff, *Phys. Rev. B* **42**, 6736 (1990).

[12] J. S. Gyanchandani, S. C. Gupta, S. K. Sikka, and R. Chidambaram, *J. Phys.: Condens. Matter* **2**, 6457 (1990).

[13] J. C. Jamieson, *Science* **140**, 72 (1963).

[14] Y. K. Vohra, S. K. Sikka, S. N. Vaidya, and R. Chidambaram, *J. Phys. Chem. Solids* **38**, 1293 (1977).

[15] L. C. Ming, M. H. Manghnani, and K. W. Katahara, *Acta. Metall.* **29**, 479 (1981).

[16] S. K. Sikka, Y. K. Vohra, and R. Chidambaram, *Prog. Mater. Sci.* **27**, 245 (1982).

[17] Y. K. Vohra and P. T. Spencer, *Phys. Rev. Lett.* **86**, 3068 (2001).

[18] Y. Akahama, H. Kawamura, and T. Le Bihan, *Phys. Rev. Lett.* **87**, 275503 (2001).

[19] V. A. Zilbershtein, G. I. Nosova, and E. I. Estrin, *Fiz. Metal. Metalloved.* **35**, 584 (1973).

[20] D. Errandonea, Y. Meng, M. Somayazulu, and D. Häusermann, *Physica B* **355**, 116 (2005).

[21] R. G. McQueen, S. P. Marsh, J. W. Taylor, J. N. Fritz, and W. J. Carter, *High Velocity Impact Phenomena*, edited by R. Kinslow, (Academic Press, New York, 1970), pp. 294-417.

[22] A. R. Kutsar, M. N. Pavlovskii, and V. V. Komissarov, *JETP Lett.* **35**, 108 (1982).

[23] R. F. Trunin, G. V. Simakov, A. V. Medvedev, *High Temp.* **37**, 851 (1999).

[24] C. W. Greeff, D. R. Trinkle, and R. C. Albers, *J. App. Phys.* **90**, 2221 (2001).

[25] E. Cerreta, G. T. Gray III, A. C. Lawson, T. A. Mason, and C. E. Morris, *J. App. Phys.* **100**, 013530 (2006).

[26] R. Ahuja, L. Dubrovinsky, N. Dubrovinskaia, J. M. Osorio Guillen, M. Mattesini, B. Johansson and T. Le Bihan, *Phys. Rev. B* **69**, 184102 (2004).

[27] D. R. Trinkle, R. G. Hennig, S. G. Srinivasan, D. M. Hatch, M. D. Jones, H. T. Stokes, R. C.

Albers, and J. W. Wilkins, *Phys. Rev. Lett.* **91**, 025701 (2003).

[28] D. R. Trinkle, D. M. Hatch, H. T. Stokes, R. G. Hennig, and R. C. Albers, *Phys. Rev. B* **72**, 014105 (2005).

[29] R. G. Hennig, T. J. Lenosky, D. R. Trinkle, S. P. Rudin, and J. W. Wilkins, *Phys. Rev. B* **78**, 054121 (2008).

[30] R. G. Hennig, D. R. Trinkle, J. Bouchet, S. G. Srinivasan, R. C. Albers, and J. W. Wilkins, *Nature Mat.* **4**, 129 (2005).

[31] K. D. Joshi, G. Jyoti, S. C. Gupta, and S. K. Sikka, *Phys. Rev. B* **65**, 052106 (2002).

[32] A. L. Kutepov and S. G. Kutepova, *Phys. Rev. B* **67**, 132102 (2003).

[33] A. K. Verma, P. Modak, R. S. Rao, B. K. Godwal, and R. Jeanloz, *Phys. Rev. B* **75**, 014109 (2007).

[34] Y. -J. Hao, L. Zhang, X. -R. Chen, Y. -H. Li, and H. -L. He, *Sol. Stat. Commun.* **146**, 105 (2008).

[35] Z. G. Mei, S. L. Shang, Y. Wang, and Z. -K. Liu, *Phys. Rev. B* **80**, 104116 (2009).

[36] C. E. Hu, Z. Y. Zeng, L. Zhang, X. -R. Chen, L. -C. Cai, and D. Alfè, *J. App. Phys.* **107**, 093509 (2010).

[37] Goodfellows, Private Communication.

[38] A. Dewaele, P. Loubeyre, and M. Mezouar, *Phys. Rev. B* **70**, 094112 (2004).

[39] A. Dewaele, F. Datchi, P. Loubeyre, and M. Mezouar, *Phys. Rev. B* **77**, 094106 (2008).

[40] A. P. Hammersley, S. O. Svensson, M. Hanfland, A. N. Fitch, and D. Häusermann, *High Press. Res.* **14**, 235 (1996).

[41] S. Desgreniers and K. Lagarec, *J. App. Cryst.* **27**, 432 (1994).

[42] T. J. B. Holland and S. A. T. Redfern, *Mineral. Mag.* **61**, 65 (1997).

[43] P. Vinet, J. Ferrante, J. Rose, and J. Smith, *J. Geophys. Res.* **92**, 9319 (1987).

[44] S. J. Clark, M. D. Segall, C. J. Pickard, P. J. Hasnip, M. I. J. Probert, K. Refson, and M. C. Payne, *Z. Kristallogr.* **220**, 567 (2005).

[45] J. P. Perdew , K. Burke & M. Ernzerhof *Phys. Rev. Lett.* **77**, 3865 (1996).

[46] A. Zunger, S. -H. Wei, L. G. Ferreira and J. E. Bernard *Phys. Rev. Lett.* **65,** 353 (1990).

[47] B. E. Tegner, L. G. Zhu, and G. J. Ackland, *Phys. Rev. Lett.* submitted (2012).

[48] W. Hume-Rothery, G. W. Mabbott and K. M. Channel-Evans, *Phil. Trans. R. Soc. A* **233**, 1 (1934).